Eur. Phys. J. E (2011) **34**: 51
DOI 10.1140/epje/i2011-11051-6

THE EUROPEAN PHYSICAL JOURNAL E

Regular Article

Reversible sphere-to-lamellar wetting transition at the interface of a diblock copolymer system

J.L. Carvalho[1], M.V. Massa[1,a], S.L. Cormier[1], M.W. Matsen[2], and K. Dalnoki-Veress[1,b]

[1] Department of Physics & Astronomy and the Brockhouse Institute for Materials Research, McMaster University, Hamilton, ON, Canada
[2] School of Mathematical and Physical Sciences, University of Reading, Whiteknights, Reading, UK

Received 9 February 2011 and Received in final form 2 May 2011
Published online: 24 May 2011 –

Abstract. We use ellipsometry to investigate a transition in the morphology of a sphere-forming diblock copolymer thin-film system. At an interface the diblock morphology may differ from the bulk when the interfacial tension favours wetting of the minority domain, thereby inducing a sphere-to-lamella transition. In a small, favourable window in energetics, one may observe this transition simply by adjusting the temperature. Ellipsometry is ideally suited to the study of the transition because the additional interface created by the wetting layer affects the polarisation of light reflected from the sample. Here we study thin films of poly(butadiene-ethylene oxide) (PB-PEO), which order to form PEO minority spheres in a PB matrix. As temperature is varied, the reversible transition from a partially wetting layer of PEO spheres to a full wetting layer at the substrate is investigated.

1 Introduction

Bulk diblock copolymer systems are generally thought to be well understood [1–4]. Such systems, made up of two covalently bonded chemically distinct linear polymer chains, exhibit a multitude of micro-phase–separated structures. These structures form due to the tendency of the two blocks to segregate under the frustration of the covalent bond which sets the lengthscale of the structures. When these materials are confined as in the case of thin films, the desire to balance surface and interfacial energetics, as well as commensurability of the structures within the confining dimension can lead to rich and unexpected morphologies [5–8]. The observation of exotic structures is especially prevalent as the degree of confinement approaches the length scale of the domain size within the ordered structure. For example, recent experimental and theoretical studies have explored equilibrium morphologies of diblocks confined to cylindrical pores [9–11] and droplets [12–14]. With decreasing length scales novel structures, vastly different from the bulk system, emerge. Much work has been carried out on symmetric diblocks, where both blocks are similar in length, under confinement. This simplest system results in a lamellar morphology in the bulk. The interplay between commensurability of the lamellae, surface energetics, and confinement to thin films is fairly well understood [5–8]. Asymmetric diblock systems, where one of the blocks is significantly shorter than the other, can result in cylindrical, spherical and even more complex morphologies in the bulk [1–4]. In confinement, the additional constraint can provide even richer phase behaviour [10,15], particularly when the minority block preferentially segregates to the boundaries [6].

Surface interactions can greatly influence ordering for thin-film systems [5–8,11,15–22]. In the simplest case, surface-induced ordering manifests itself as a wetting layer of the block with the more favourable surface energy at the film boundaries [5–8]. More complicated mixed morphologies have also been found to be stable including mixed lamellar orientations that are parallel and perpendicular to the substrate surface, or lamellae that persist for a number of layers from the boundary with curved morphologies away from the surface [5–7,15–17,20]. Theoretical studies on thin films of cylinder- and sphere-forming diblock systems have shown that strong surface fields can stabilize lamellar phases far from the boundary despite the stretching-penalty incurred in deforming the bulk equilibrium structure [5,15]. Further studies have suggested that mixed-lamellar morphologies, as equilibrium phases, are only stable when there is a degree of asymmetry in the volume fraction [6] or surface energetics [20]. As one probes even thinner films, the additional constraints of confinement and surface interactions can result in further differences between how bulk and thin films order. Recently, Kramer and coworkers investigated a transition from two- to three-dimensional packing of the domain structures in

[a] *Current address:* Department of Physics, University of Guelph, Guelph, ON, Canada.
[b] e-mail: dalnoki@mcmaster.ca

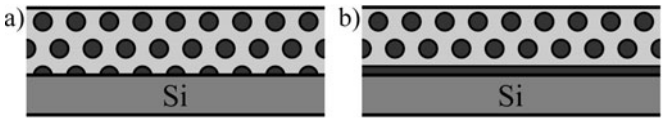

Fig. 1. Schematic of the substrate-induced transition. As the diblock film of minority (PEO) spheres within a matrix (PB) is cooled, the layer of spherical caps (a) reorders into a full wetting layer covering the substrate (b).

a highly asymmetric diblock [23]. For sphere-forming systems, domains are known to pack in a body-centered cubic (bcc) lattice in the bulk, while a hexagonal (hex) lattice is preferred in very thin films. These two ordered morphologies minimize packing frustration for their respective constraints [4,23].

Let us consider the case of an asymmetric, sphere-forming, diblock copolymer where the minority block "a" has a preference for the substrate compared to the matrix "b". This is equivalent to stating that $\gamma_{a,s} < \gamma_{b,s}$, where γ is the interfacial tension of either block with the substrate as denoted by the subscripts. There are two contributions to the free energy which determines the morphology observed at the interface. If the substrate surface energy term dominates, that is, $\Delta\gamma = (\gamma_{b,s} - \gamma_{a,s})$ is large, then there will be a wetting layer of the "a"-block at the substrate at the cost of the preferred spherical morphology in the bulk. As a minimal constraint, $\Delta\gamma > \gamma_{a,b}$, where $\gamma_{a,b}$ is the tension at the diblock a-b interface [5,24]. Entropy favours a curved a-b interface for the asymmetric diblock case, thereby maximising the configurations available to the blocks while maintaining micro-phase separation. If the entropic term which drives spherical morphology in the bulk system dominates, then the free energy is minimised by placing the substrate interface such that it bisects the domains. Figure 1 is a schematic representation of these two cases. Furthermore, we can imagine a system where at high temperatures spherical caps are found (entropy dominates) which transition to a full wetting layer upon cooling (the enthalpic interfacial tension term dominates).

Here we present a study of asymmetric sphere-forming diblock poly(butadiene-ethylene oxide) (PB-PEO) thin films on a Si substrate. As we will show, this system exhibits a fortuitous balance between the enthalpic and entropic interactions such that the transition between the sphere and lamella state at the substrate interface, appears within an experimentally accessible temperature window. To the best of our knowledge these are the first direct measurements of this substrate induced transition.

2 Experiment

Poly(1-4 addition butadiene-ethylene oxide) was purchased from Polymer Source Inc. (Canada). The PB-PEO had number averaged molecular weights of $M_n(\mathrm{PB}) = 26\,\mathrm{kg/mol}$ and $M_n(\mathrm{PEO}) = 7.5\,\mathrm{kg/mol}$ for the two blocks, and a polydispersity index of 1.06. Thin films were spin-cast from dilute toluene solutions (0.5 to 4 wt.%) onto clean Si substrates with the native oxide layer, which had been UV ozone treated to remove any remaining organic contaminants. Film thicknesses, h, from 35 nm to 200 nm were obtained by varying the solution concentration and spin speed. Samples were annealed for over 20 hours in vacuum at 90 °C. This temperature is well below the bulk order-disorder transition temperature for this system ($T_{\mathrm{ODT}} > 220\,^{\circ}\mathrm{C}$ [25]), resulting in a micro-phase–separated morphology of PEO minority spheres (14 nm radius [26]) in a PB matrix. The ordered structure was confirmed with atomic force microscopy (AFM) of the top surface. The PB-PEO system satisfies the conditions for observing the substrate-induced morphology transition described above. The surface energy of PB is lower than PEO resulting in a PB layer at the free surface [27]. From wetting/dewetting experiments, we have found that the minority PEO block has a greater preference for the Si substrate and there is an energetic drive for PEO to wet the substrate. Thus, the PB-PEO diblock system exhibits asymmetric boundary conditions: PEO has a preference for the substrate, while PB favours segregation to the air interface (see schematic in fig. 1 where the dark domains represent PEO, and the grey matrix is the PB).

After annealing the samples, they were transferred to the ellipsometer. Measurements were carried out on a custom-built, single-wavelength (632.8 nm) self-nulling ellipsometer (for further details see previous ellipsometry investigations into crystallisation of the same PB-PEO system [28,29]). In the self-nulling mode of ellipsometry a polariser is rotated to angle P such that the emerging linear polarised light passes through a quarter wave plate onto the sample at some angle of incidence (50° was used in this case). The polariser is rotated to produce elliptically polarised light before the sample which emerges as linearly polarised after reflection from the film covered substrate. Another polariser, called the analyser is then rotated to an angle, A, to null the intensity at the detector [30]. In all experiments, the polariser and analyser angles, P and A, were measured as a function of temperature, T, and then converted to film thickness, h, and refractive index, n, using the standard equations of ellipsometry [30]. Temperature control on the ellipsometer was achieved with a modified optical microscope heating stage (Linkam, THMS 600, United Kingdom) flushed with dry nitrogen. Samples were annealed at 70 °C for 20 min prior to measurement, cooling to −18 °C, held for 5 mins, then heated back to 70 °C. This temperature range is above the glass transition for bulk PB ($T_g < -40\,^{\circ}\mathrm{C}$ [31]) and the crystal nucleation temperature for PEO spheres of this size ($T_c = -21\,^{\circ}\mathrm{C}$, as measured by ellipsometry [28,29]). Within this temperature range both block components were in the amorphous melt state. We note that the fact that both ordered phases remain fluid within the temperature window required for the transition to take place makes the measurement of the change in morphology possible. For most measurements heating and cooling was carried out at 1 °C/min. To probe the dynamics of the morphological transition, heating and cooling rates from 0.02 °C/min to 5 °C/min were used.

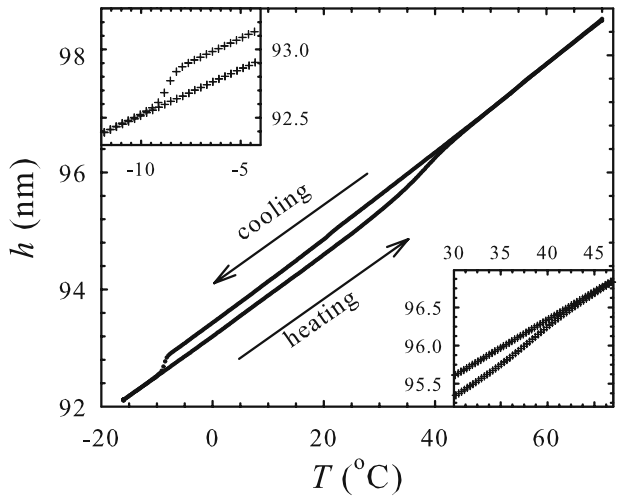

Fig. 2. A typical ellipsometry experiment. The sample has been cooled from 70 °C to −18 °C. At −9 °C, a deviation in the cooling data can be seen, with a reverse transition at ∼ 40 °C upon heating.

3 Results and discussion

Though ellipsometry is a standard experimental tool, we discuss a few of the details crucial to the work presented. The conversion of the angles measured in ellipsometry to h and n is model dependent [30]. One of the simplest models used is the assumption of a single uniform film covering a substrate: the refractive index of the film does not vary in the film normal direction, $n(z) = n$, where z is the distance from the substrate. In the case of a non-uniform film, for example if there is a gradient in the index of refraction $\mathrm{d}n/\mathrm{d}z \neq 0$, then the "uniform film" model does not hold. An extreme example of a gradient in the index is that of a bilayer film. Since polarisation of light is affected by reflections from the additional interface in a bilayer film, a bilayer film model must be used [30]. While the films studied here are not of uniform composition, as long as we can treat the domains of PEO as much smaller than the wavelength of light, a constant index of refraction describes the system with an index intermediate to that of the PEO and PB.

In the schematic shown in fig. 1(a), the uniform-film model is an excellent assumption because the PEO domains are much smaller than the wavelength of light. Furthermore, the footprint of the laser light illuminates an area of $\sim 3\,\mathrm{mm}^2$ containing about 10^{10} domains. That the uniform-film model is a good assumption for samples of the sort shown in fig. 1(a) has been well established in previous studies of crystal nucleation in the minority PEO spheres [28,29]. Clearly, if the sample undergoes a morphological transition at the buried interface as shown in fig. 1(b), the uniform-film assumption is no longer valid. In that case, the sample must be treated as a bilayer because of the change in polarisation induced by the PEO wetting layer.

In fig. 2 we show a typical ellipsometry experiment identifying the substrate-induced morphological transition. In this figure, measured $P(T)$ and $A(T)$ data have been converted to film thickness $h(T)$ (shown), and refractive index $n(T)$ (not shown), using the uniform-film model. As the film is cooled from 70 °C, the film contracts at a constant thermal expansion rate as expected, thus resulting in a constant slope [28,29]. At −9 °C a sharp deviation occurs, followed by a return to the initial contraction rate down to −18 °C. On subsequent heating, the film expands with the same expansion coefficient until a broader deviation occurs at 40 °C. AFM of the free surface layer before and after the morphological transition upon cooling indicates that the phase-separated spherical morphology is unaltered by the transition. The fact that the expansion coefficient does not change following the two transitions rules out a crystallisation mechanism as being responsible for the observed deviations. We have previously shown that crystallisation of some component of the phase-separated film results in a measurable change in the expansion coefficient due to the fact that following crystallisation the film contains a solid component [28].

We now turn to the origin of the transitions in *apparent* film thickness. As will be made more clear below, the apparent change in thickness, Δh, occurs at the morphological transition from spherical caps of PEO at the substrate interface to a wetting layer of PEO. Simply put, while the uniform-film model used is valid upon cooling down to −9 °C (fig. 1(a)), below the sphere-to-lamella transition a bilayer model must be used (fig. 1(b)). While the difference is small, corresponding to a mere $\sim 0.2\,\mathrm{nm}$, it is clearly measurable with ellipsometry (see insets of fig. 2 where the individual data points are visible). Furthermore, the fact that the data at the beginning and end of the experiment are identical indicates that instrumental drift, or irreversible changes in the sample, can be ruled out.

Further evidence that the sudden deviation in film thickness is the result of the wetting transition is provided in fig. 3. Here we show data for the magnitude of the apparent thickness and index change, Δh and Δn, for experiments on films ranging from 35 nm to 200 nm. It can be seen that, depending on the overall film thickness, an apparent increase or decrease in film thickness occurs as a result of the transition. Again, these results do not support a crystallisation-based mechanism for the transition, as crystallisation in some portion of the film will always result in a contraction of the film. Such a contraction can be seen in our previous work related to this PB-PEO system [28]. An expansion of the film upon crystallisation is not consistent with what is known about polymer crystallisation. For all these measurements, Δh and Δn are the result of using the uniform-film model which is only valid at temperatures above the transition. Below the transition a bilayer model must be used. To clarify, $\Delta h \sim -0.2\,\mathrm{nm}$ is the vertical difference between the two lines in fig. 2 for the 96 nm film which represents a single data point in fig. 3.

Knowing that the sudden transitions in $h(T)$ and $n(T)$ are simply an artefact of using the uniform-film model in a temperature range where the bilayer film model must be used enables a direct verification. P and A values were simulated using standard equations of ellipsometry and

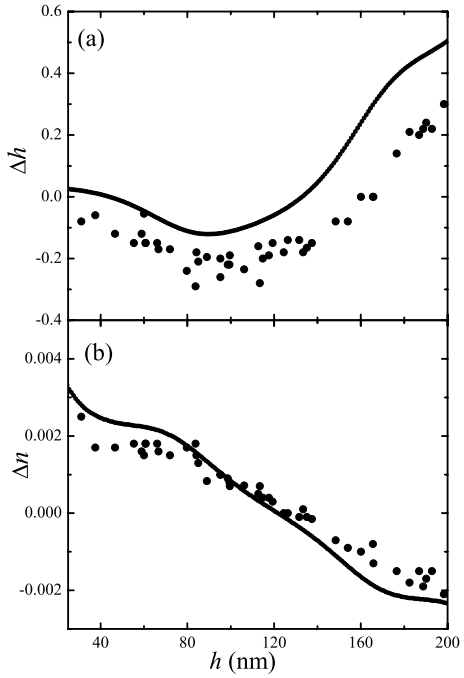

Fig. 3. Changes in the apparent thickness, Δh (a), and the apparent refractive index, Δn (b), as a function of film thickness. Discrete points were measured experimentally, smooth curve represents simulated data.

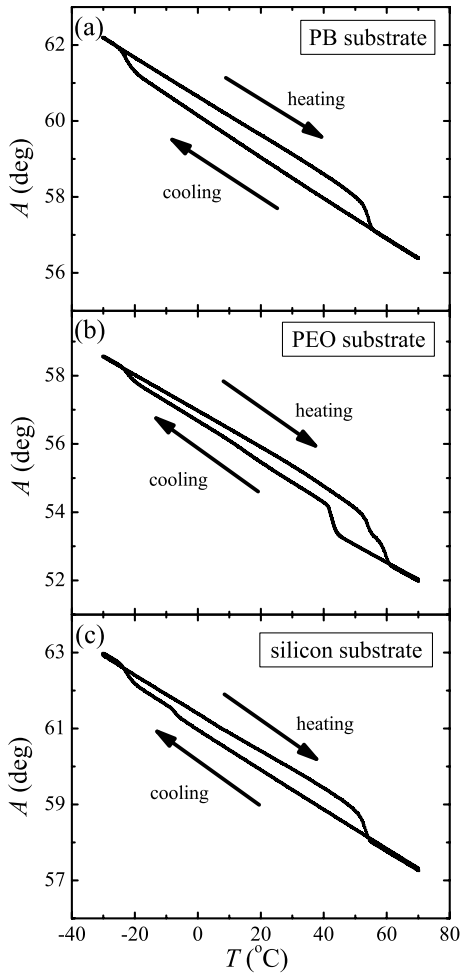

Fig. 4. The analyzer angle, $A(T)$, for PB-PEO films prepared on a PB substrate (a), a PEO substrate (b), and on a Si substrate (c). For all three plots crystallisation of the PEO domains can be seen to take place below $-20\,^{\circ}$C, with subsequent melting upon heating the film above $50\,^{\circ}$C. Additionally, in (b) the PEO substrate layer can be seen to crystallise at $43\,^{\circ}$C with subsequent melting upon heating the film above $59\,^{\circ}$C. In both (a) and (b), the morphological transition evident at $-8\,^{\circ}$C on the Si substrate (c), is *not* seen either upon cooling (sphere-to-lamella at $\sim -10\,^{\circ}$C) or heating (lamella-to-sphere at $\sim 40\,^{\circ}$C). The substrate properties can turn off the observation of the reversible transition (note that for (c) the morphological transition upon heating is not seen because the PEO spheres are in the crystalline state and cannot rearrange until in the melt state $\sim 53\,^{\circ}$C).

reasonable values for substrate and film refractive indices. Two different geometries were considered corresponding to the two models shown in fig. 1: 1) a homogeneous uniform PB-PEO film on a Si substrate; and 2) a bilayer film consisting of a homogenous uniform PB-PEO layer with a 2.5 nm wetting layer of PEO (all index of refraction parameters have been measured with ellipsometry). A 2.5 nm layer was chosen as an estimate for the lamellar layer thickness based on knowledge of the spherical domain size and assuming volume is conserved in going from a half-sphere to a lamellar wetting layer. For both sets of simulated data, values for thicknesses of $35 < h < 220$ nm were generated in 1 nm increments. The simulated h and n values using model 2) were subtracted from model 1) and respectively plotted as a function of film thickness as the solid line in fig. 3. Thus, these simulated values of Δh and Δn as a function of film thickness represent the artefact induced by assuming a single homogeneous film model in the regime where a wetting layer exists.

In fig. 3, there is good agreement between the simulated and experimental data. The small systematic difference can be attributed to the simplicity of the model used for the simulation compared to the actual system. The agreement confirms the schematic of fig. 1 and indicates that the apparent changes observed in h and n are indeed due to the morphological transition at the buried interface.

Having established that the transition in morphology is induced by the substrate, it is clear that the transition is sensitive to surface energy of the substrate, or more precisely $\Delta\gamma = (\gamma_{\mathrm{PB,Si}} - \gamma_{\mathrm{PEO,Si}})$. Thus, by tuning the substrate surface energy, we should be able to "turn off" the reversible transition. We have tuned $\Delta\gamma$ in two ways. First, we have made the substrate very unfavourable for the PEO block by using a thin adsorbed PB ($M_n \sim 75$ kg/mol) film spincast onto Si as our substrate, with the diblock film then spun on top. In fig. 4(a) is shown the analyser angle A as a function of temperature. Upon cooling the film, no deviation related to the ordering transition is seen at $\sim -10\,^{\circ}$C. Rather a sudden change is seen at $\sim -23\,^{\circ}$C consistent with the crystallisation of

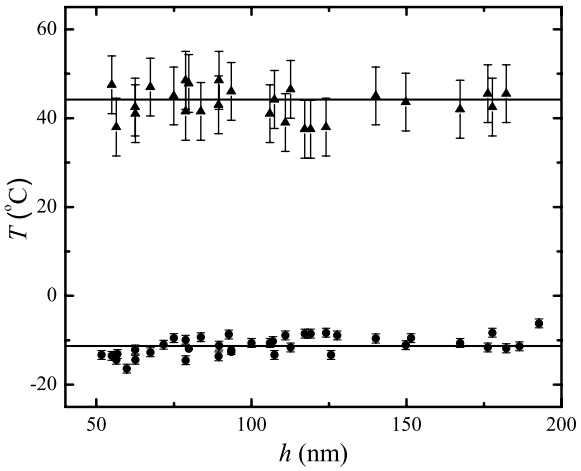

Fig. 5. Transition temperature as a function of film thickness. Round data points represent the sphere-to-lamellar transition that takes place upon cooling the sample. Triangles represent the reverse lamellar-to-sphere transformation after subsequent heating. A large hysteresis is evident between the two data sets.

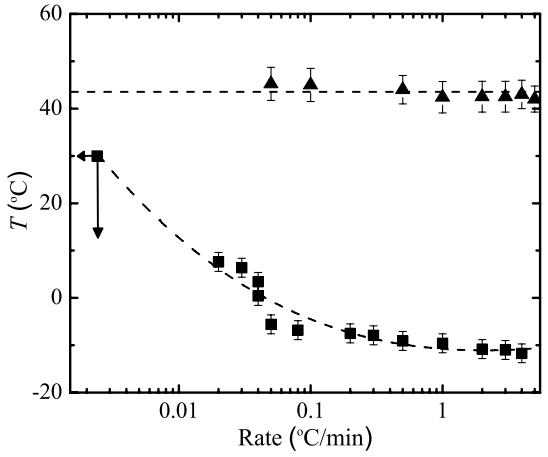

Fig. 6. Rate dependence of the substrate-induced transition. For the sphere-to-lamella transition (squares), samples were cooled from 70 °C to −18 °C. For the lamella-to-sphere transition (triangles), samples were first cooled at a fixed rate of 4 °C/min from 70 °C to −18 °C to ensure identical initial conditions, held for 5 mins and then heated with the range of rates indicated. The lowest rate data point is a "pseudo-infinitely slow" measurement and provides an upper bound as explained in the text.

PEO [28,29]. Likewise, upon heating only the melting of the crystal domains is seen at $\sim 55\,^{\circ}$C. By making the substrate far more favourable for the PB block, $\Delta\gamma < 0$, there is no drive to form a wetting layer and the transition has been inhibited. In the second instance, we have made the substrate much more favourable for the PEO block by spincasting a thin PEO film ($M_n \sim 10^3$ kg/mol) onto Si and subsequently coating the diblock film. These data are shown in fig. 4(b). Again, no transition related to morphological reordering is seen at $\sim -10\,^{\circ}$C upon cooling, or at $\sim 40\,^{\circ}$C upon heating. For this system, the PEO block obviously has an even larger affinity for the PEO substrate than for the case of bare Si, thereby shifting the transition temperature window. The driving force to form a lamellar wetting layer is large enough that a layer should be present at all temperatures, consistent with the fact that the transition is no longer evident at any temperature for this particular case. We note that the transitions that are observed in the data are all related to the crystallisation of the PEO (see figure caption) [28,29].

In fig. 5, we have plotted the temperature, at which both the sphere-to-lamella (cooling) and lamella-to-sphere (heating) transitions take place as a function of film thickness. Notable features of the data in this plot are: 1) the considerable scatter in the data, 2) within the range studied there is no film thickness dependence, and 3) there is significant hysteresis in the reversible transition. The scatter in the temperature of the transition upon heating (lamella-to-sphere) can be attributed to the broad nature of the transition (see fig. 2), and is indicated by the large error bars for these data points. However, when cooling, the sphere-to-lamella transition is very sharply defined (see fig. 2). Thus, we cannot attribute the scatter in these data points to measurement uncertainty. Rather, we suspect that this scatter is due to small variations in the surface energy of the Si substrate at the time the films were prepared, despite our best efforts toward consistency. Given that we have been able to effectively turn off the transition by tuning the substrate surface energy, it seems reasonable that variations in surface energy will result in scatter in the transition temperature. While the same surface energy variations are also likely a factor in the scatter of the lamella-to-sphere transition upon heating, this is overwhelmed by the breadth of the transition resulting in a larger measuring uncertainty. Tsarkova and co-workers have also noted the need for systematic cleaning procedures to better achieve reproducibility in a study of phase transitions for a cylinder-forming diblock system that is directed by the substrate [21]. Regardless, the sphere-to-lamella transition occurs at $-11 \pm 2\,^{\circ}$C upon cooling with the reverse transition at $43 \pm 4\,^{\circ}$C.

From fig. 5, it is evident that there is large hysteresis between the two transitions. To determine if this hysteresis is simply the result of kinetics, or an underlying difference in the sphere-to-lamella *versus* lamella-to-sphere transition, cooling and heating rates were varied from 0.02 °C/min to 5 °C/min, and the effect on transition temperature measured (see fig. 6). There does not appear to be any measurable rate dependence for the lamella-to-sphere transition when heating. In contrast the sphere-to-lamella transition moves to higher temperatures with slower cooling rates. It should be noted that even for the slowest cooling rate of 0.02 °C/min, there is a hysteresis of $\sim 35\,^{\circ}$C. While slower rates were not experimentally feasible, we have been able to conduct "pseudo-infinitely" slow experiments which provide a bound on the transition. A film was cooled at 1 °C/min to 30 °C and held for 4 days. Upon subsequent heating, there was no lamella-to-sphere transition indicating that the sphere-to-lamellar transition had not occurred during that time. Though no transition could be measured, this observation provides an

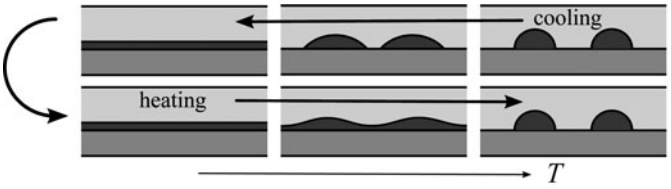

Fig. 7. Schematic diagram of a potential pathway for the the transition from sphere-to-lamella upon cooling and lamella-to-sphere upon heating.

upper bound on the transition if it could occur at 30 °C. The upper bound "pseudo-infinite" data point is shown at (0.0023 °C/min, 30 °C) (the upper bound on the rate is obtained as follows: since no transition occurred while holding at 30 °C for 4 days, then if a transition could occur at this temperature, the rate must be less than than (43 °C − 30 °C)/4 days). We speculate that the hysteresis that is maintained even for very slow rates indicates a fundamental difference in the thermodynamics of the transition when cooling and heating. The hysteresis may be the result of different pathways for the sphere-to-lamella and lamella-to-sphere transition. In fig. 7 we construct a tentative diagram of the transition. Starting from high temperature the sample is cooled and the interfacial term that drives spreading of the minority domains dominates. The minority domains increase contact area with the substrate, growing until adjacent domains touch at which point the wetting layer is established. The continuous change upon cooling suggests there is no activation barrier to the transition. During the reverse cycle, the situation is different. In order for domains to form, the wetting layer interface must undulate at the cost of an increased interfacial area, suggesting an activation barrier. Fluctuations of the interface must grow until they touch the substrate at which point the transition to spherical cap domains can occur. The existence of an activation barrier is also consistent with the observation that the temperature range over which the transition takes place is broad (compare insets of fig. 2). We note the strong analogy to the spinodal and binodal points in the phase separation of binary blends.

Lastly, we comment in more detail on the origin of the transition. As discussed above, the conditions for observing the transition from sphere-to-lamella upon cooling requires the interfacial energy of the minority domain with the substrate, $\gamma_{a,s}$, to be less than that of the matrix on the substrate, $\gamma_{b,s}$. Consider a simple liquid droplet with surface tension γ_l, on a substrate with surface tension γ_s, the spreading parameter is defined as $S = \gamma_s - (\gamma_{s,l} + \gamma_l)$, where $\gamma_{s,l}$ is the interfacial tension of the solid-liquid interface [32]. The droplet will wet the substrate when $S > 0$. By analogy, we arrive at a necessary but not sufficient condition that $\Delta\gamma = \gamma_{b,s} - \gamma_{a,s} > \gamma_{a,b}$ for the spheres to transform into a lamella. As pointed out by Turner and co-workers [5], for it to be sufficient, the reduction in surface energy must compensate both the increase in *a*-*b* interfacial area and the entropic cost associated with deforming the *a*-*b* interfacial curvature, which favours a spherical cap for the asymmetric diblock case. Hence the sphere-to-lamella transition requires the energy difference,

$$\Delta\Omega = n\Delta F - p(\gamma_{b,s} - \gamma_{a,s}), \tag{1}$$

to become negative, where n is the number of molecules involved in the transition per unit area, ΔF is the free-energy difference per molecule between the sphere and lamella morphologies, and p is a geometrical factor specifying the fraction of the substrate covered by the matrix component of the sphere morphology.

Interfacial tensions are typically not strongly dependent on temperature, so we need to understand the temperature dependence of transforming the *a*-*b* interface, $n\Delta F$. For the system studied, we are well below the order-disorder transition temperature of the diblock and can therefore apply strong-segregation theory (SST) (see [3] for detailed discussion of the scaling that is to follow). According to SST, the free energy per chain varies as $F/T \sim \chi^{1/3}$, where $\chi \sim 1/T$ is the Flory-Huggins parameter describing the interaction between the blocks. The temperature scaling per molecules is then $F \sim T^{2/3}$. The number of molecules, n, involved in the transition is proportional to the characteristic domain size, which scales as $\chi^{1/6} \sim T^{-1/6}$ (see eq. (3) in [3]). Thus the free energy per unit area of the wetting layer varies as $nF \sim T^{1/2}$. Since the free energy of both the spherical caps with ideal curvature and the wetting layer scale as $\sim T^{1/2}$, so does their difference, $n\Delta F$. Keeping only the temperature dependence, we have

$$\Delta\Omega \sim c\sqrt{T} - p(\gamma_{b,s} - \gamma_{a,s}), \tag{2}$$

where c and p are positive constants and the interfacial tensions only have a weak temperature dependence. From eq. (2) we can clearly see that as the temperature is decreased the interfacial term dominates at the expense of curvature and the sphere-to-lamella transition is favoured. Clearly, a very serendipitous balance of the contributions in eq. (2) is required in order to observe the transition within the temperature range accessible to experiment.

4 Conclusions

Here we have used ellipsometry to probe a surface-induced transition in the morphology of an asymmetric PB-PEO diblock. At high temperatures the bulk-like morphology is found at the substrate: PEO spherical caps of the minority domain cover the interface, since the PEO has a more favourable interaction with the substrate than does PB. However as temperature decreases, and with it the entropic penalty associated with distortion of the curved spherical interface, the surface energies dominate. At low temperature a thin wetting layer of PEO has a lower free energy than spherical caps. Since ellipsometry is very sensitive to the additional buried interface provided by the wetting layer, the sphere-to-lamella transition is easily measured. Furthermore, upon subsequent heating the reverse transition occurs with significant hysteresis between

the transition upon cooling and upon heating. The reversible surface directed transition between the spherical cap and wetting layer morphologies is strongly dependent on the surface energy of the substrate. We have shown that by modifying the energetics the morphological transition can be turned off.

Financial support from NSERC of Canada is gratefully acknowledged.

References

1. F.S. Bates, G.H. Fredrickson, Annu. Rev. Phys. Chem. **41**, 525 (1990).
2. G.H. Fredrickson, F.S. Bates, Annu. Rev. Mater. Sci. **26**, 501 (1996).
3. M. Matsen, F. Bates, J. Chem. Phys. **106**, 2436 (1997).
4. M. Matsen, J. Phys.: Condens. Matter **14**, R21 (2002).
5. M. Turner, M. Rubinstein, C. Marques, Macromolecules **27**, 4986 (1994).
6. M. Matsen, J. Chem. Phys. **106**, 7781 (1997).
7. M. Fasolka, A. Mayes, Annu. Rev. Mater. Res. **31**, 323 (2001).
8. P. Green, R. Limary, Adv. Colloid Interface Sci. **94**, 53 (2001).
9. H. Xiang, K. Shin, T. Kim, S. Moon, T. McCarthy, T. Russell, Macromolecules **37**, 5660 (2004).
10. H. Xiang, K. Shin, T. Kim, S. Moon, T. McCarthy, T. Russell, J. Polym. Sci., Part B: Polym. Phys. **43**, 3377 (2005).
11. B. Yu, P. Sun, T. Chen, Q. Jin, D. Ding, B. Li, A. Shi, Phys. Rev. Lett. **96**, 138306 (2006).
12. A. Croll, M. Massa, M. Matsen, K. Dalnoki-Veress, Phys. Rev. Lett. **97**, 204502 (2006) ISSN 1079-7114.
13. J. Kim, M. Matsen, Soft Matter **5**, 2889 (2009) ISSN 1744-683X.
14. T. Kim, J. Huh, C. Park, Macromolecules **43**, 5352 (2010) ISSN 0024-9297.
15. H. Tan, D. Yan, A. Shi, Macromolecules **37**, 9646 (2004).
16. P. Mansky, T. Russell, C. Hawker, M. Pitsikalis, J. Mays, Macromolecules **30**, 6810 (1997).
17. E. Huang, P. Mansky, T. Russell, C. Harrison, P. Chaikin, R. Register, C. Hawker, J. Mays, Macromolecules **33**, 80 (2000).
18. H. Huinink, J. Brokken-Zijp, M. Van Dijk, G. Sevink, J. Chem. Phys. **112**, 2452 (2000).
19. H. Yokoyama, T. Mates, E. Kramer, Macromolecules **33**, 1888 (2000).
20. M. Fasolka, P. Banerjee, A. Mayes, G. Pickett, A. Balazs, Macromolecules **33**, 5702 (2000).
21. L. Tsarkova, A. Knoll, G. Krausch, R. Magerle, Macromolecules **39**, 3608 (2006).
22. G. Stein, E. Kramer, X. Li, J. Wang, Macromolecules **40**, 2453 (2007).
23. G. Stein, E. Cochran, K. Katsov, G. Fredrickson, E. Kramer, X. Li, J. Wang, Phys. Rev. Lett. **98**, 158302 (2007).
24. Y. Li, Y. Loo, R. Register, P. Green, Macromolecules **38**, 7745 (2005).
25. Y. Huang, H. Chen, T. Hashimoto, Macromolecules **36**, 764 (2003).
26. In order to obtain the sphere radius, we used the strong-stretching theory expression for domain size as described by Matsen and Bates [3] with experimental parameters for the sphere radius and volume fractions given for an equivalent system by similar system by Huang and coworkers [25].
27. C. Vasilev, H. Heinzelmann, G. Reiter, J. Polym. Sci., Part B: Polym. Phys. **42**, 1312 (2004).
28. J. Carvalho, M. Massa, K. Dalnoki-Veress, J. Polym. Sci., Part B: Polym. Phys. **44**, 3448 (2006).
29. J. Carvalho, M. Somers, K. Dalnoki-Veress, J. Polym. Sci., Part B: Polym. Phys. **49**, 712 (2011).
30. R. Azzam, N. Bashara, S. Ballard, Phys. Today **31**, 72 (1978).
31. C. Vasilev, G. Reiter, S. Pispas, N. Hadjichristidis, Polymer **47**, 330 (2006).
32. P. de Gennes, F. Brochard-Wyart, D. Quéré, *Capillarity and Wetting Phenomena* (Springer-Verlag, New York Inc., 2002).